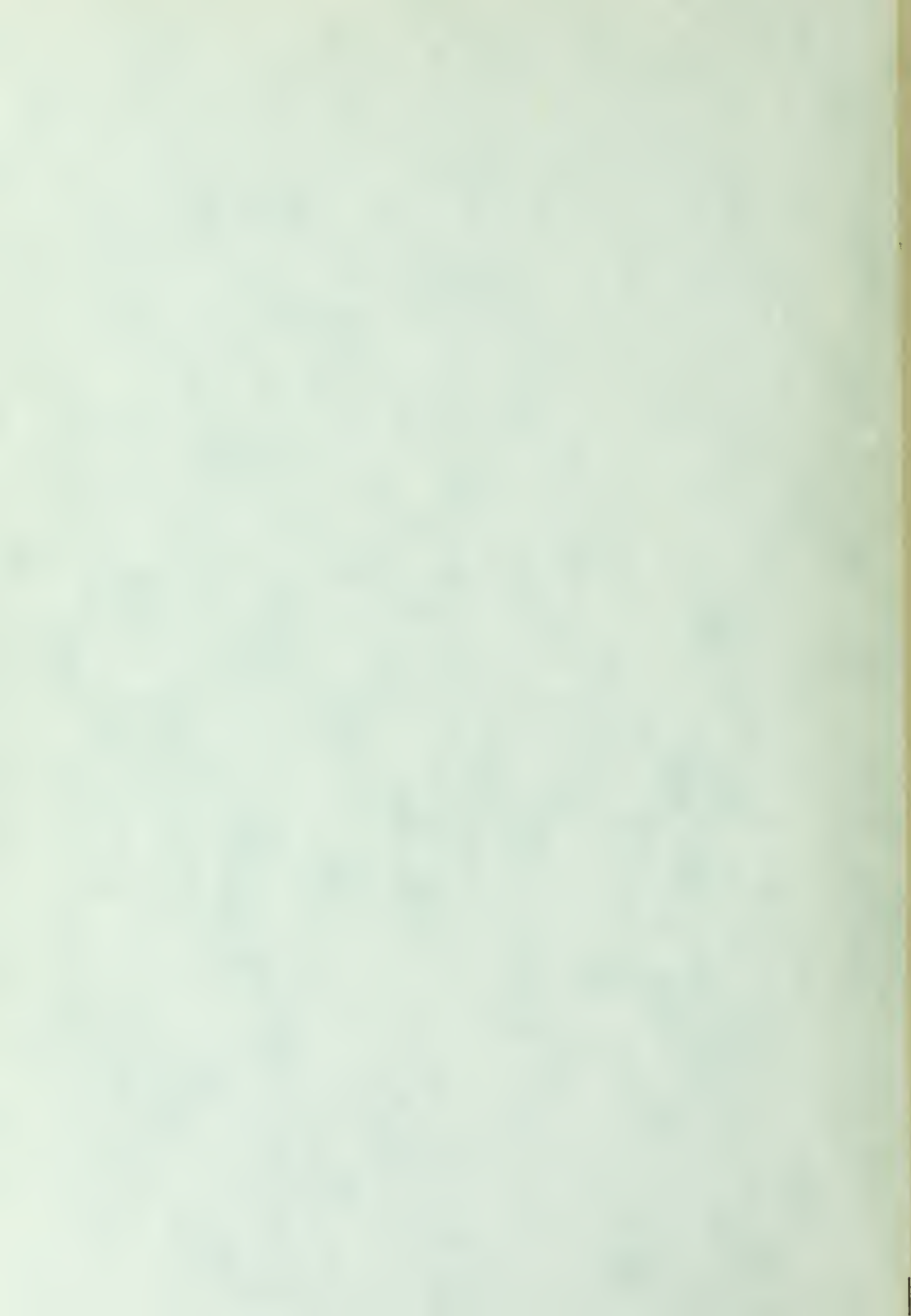


A LOW IMPEDANCE HIGH CURRENT ULTRASONIC  
SIGNAL SOURCE FOR FERRORESONANCE STUDY.

by

John Reynolds Pratchios



# United States Naval Postgraduate School



## THESIS

A LOW IMPEDANCE HIGH CURRENT  
ULTRASONIC SIGNAL SOURCE  
FOR FERRORESONANCE STUDY

by

John Reynolds Pratchios

September 1970

*This document has been approved for public release and sale; its distribution is unlimited.*

T137597



A Low Impedance High Current  
Ultrasonic Signal Source for Ferroresonance Study

by

John Reynolds Pratchios  
Lieutenant (junior grade), United States Navy  
B.S., United States Naval Academy, 1969

Submitted in partial fulfillment of the  
requirements for the degree of

MASTER OF SCIENCE IN ELECTRICAL ENGINEERING

from the

NAVAL POSTGRADUATE SCHOOL  
September 1970



## ABSTRACT

In ferroresonant mode, a transformer is saturated and requires very high currents from the source. Previous studies of ferroresonance could not be performed effectively because of high internal impedance of the source. Introduction of transformers to improve these shortcomings would have also introduced undesirable inductive effects. In this thesis, a transistor voltage source with low internal impedance and high current delivering ability is designed and tested. The source is used to investigate an unsymmetrical mode of series resonance. Resonant circuit behavior is both qualitatively and quantitatively described.





## TABLE OF CONTENTS

I.	INTRODUCTION -----	5
II.	THE ULTRASONIC SIGNAL SOURCE -----	6
A.	DESIGNING THE SOURCE -----	6
1.	Circuit Configuration -----	6
2.	Transistor Selection and Matching -----	9
3.	Physical Consideration -----	10
B.	TESTING THE SOURCE -----	11
1.	Distortion -----	11
2.	Internal Impedance -----	12
III.	THE SERIES RESONANT CIRCUIT -----	14
A.	OBSERVATION OF THE PHENOMENON -----	14
B.	QUALITATIVE DESCRIPTION OF THE PHENOMENON ----	16
C.	QUANTITATIVE DESCRIPTION OF THE PHENOMENON ---	18
1.	Circuit Equations -----	18
IV.	CONCLUSION -----	26
	APPENDIX A -----	27
	APPENDIX B -----	30
	BIBLIOGRAPHY -----	35
	INITIAL DISTRIBUTION LIST -----	36
	FORM DD 1473 -----	37



Blank



## I. INTRODUCTION

Until the advent of high power transistors, obtaining low internal impedance signal sources with high current handling ability was virtually impossible in the ultrasonic region. With the expected frequency of ferroresonance in the neighborhood of 15 kilohertz to 25 kilohertz, the use of transformers for impedance transformation and current multiplication is impractical. The transformer inductance would limit rate-of-current changes when the ferroresonant core saturates and hysteresis effects would introduce non-linear harmonic distortion.

This circuit uses silicon transistors with both high current handling ability and high current gains while maintaining very wide frequency response. The source displays very low impedance, on the order of .25 ohm and delivers approximately 5 amperes of peak-to-peak signal current into a .1 ohm load. Distortion is held to a very low value.



## II. THE ULTRASONIC SIGNAL SOURCE

### A. DESIGNING THE SOURCE

#### 1. Circuit Configuration

Before transistors could be selected, a circuit configuration had to be decided on. For high power stages with low distortion there are two basic configurations used, both with their advantages and disadvantages. These configurations are complementary symmetry and quasi complementary symmetry. The former uses complementary PNP - NPN pairs of transistors in the output transistors, or both the drivers and an output transistors. The advantages are that no inverter stage is necessary and that there is a constant load on the driver stage on both the positive and negative swings of the output voltage. The latter is important in order to maintain linear operation and low distortion. The basic disadvantages are procurement of PNP and NPN transistors that are truly similar and the necessity for matching the transistor pairs for optimum operation. The latter circuit configuration uses the same type transistors (both either PNP or NPN) in the output stage but drives them with a complementary pair of transistors in the drive circuit. The advantages are that the output transistors are easier to match and are of the same type. The disadvantages are that the circuit is not as stable as pure complementary symmetry and distortion is higher because both halves of the input sine wave do not see the same impedance at the drivers. (Because one driver output pair is operated in a Darlington





configuration and the other pair is operated in a common emitter driving an emitter follower - the former is higher in input impedance than the latter.) In addition, biasing requirements are complicated by the NPN - NPN pair having twice the  $V_{be}$  of the PNP - NPN pair (or the PNP - PNP having twice the  $V_{be}$  of the NPN - PNP depending of the type of output transistors used).

For this application, two stages of pure complementary symmetry were chosen: a NPN - PNP pair driving a PNP - NPN pair. The circuit appears in Figure 1 Appendix A. Rather than use diodes to compensate for the potential difference between the bases of the drivers caused by the  $V_{be}$  of these transistors as is customary in most circuits of this nature, it was decided to incorporate a transistor. (Whose  $V_{be}$  would be more nearly that of the drivers than the voltage across a diode.) The transistor was used in a regulated power supply circuit known as a " $V_{be}$  multiplier" to provide the proper bias between the two bases of the transistors. In this circuit configuration, a bias can be obtained which can be tailored to what ever value is desired. The current through the transistor is chosen at a suitable value and collector-base and emitter-base resistors are chosen such that the base current is negligible compared to the current through these resistors, therefore the current through the collector-base resistor will be the same as that through the emitter-base resistor. The voltage across the emitter-base resistor, and therefore the current through it, is determined by the  $V_{be}$  of the transistor. Tailoring the ratio



of these two resistors will change the base-collector voltage and therefore the entire bias voltage. Here a potentiometer was used for complete control of the bias so that acrossover distortion could be minimized.

Various forms of predrivers were designed but testing found most of them unsatisfactory from a distortion standpoint. It was decided to feed the signal from a signal generator directly to the drivers and tailor the input impedance of the source to 600 ohms to match the output impedance of the signal generator. The signal generator was a Hewlett Packard Model 200AB which was fully capable of delivering up to 100 volts of signal if necessary. The input signal was coupled in with a normal R - C network,  $C_1$  and  $R_1$ . In addition, some signal is bypassed around the bias supply to the voltage divider consisting of  $R_4$  and  $R_5$ . This is to counter only bias changes caused by the unbypassed collector resistors  $R_8$  and  $R_9$  which might alter bias with signal.

To insure distortion free operation and stability, negative feedback was applied via a series R - C network comprised of  $C_4$  and  $R_{10}$  from the output to the input. Since the source was capable of delivering large amplitude signals, a great deal of feedback was able to be applied to reduce distortion. In addition, since the feedback is of the shunt type, the additional benefit of further reduced output impedance was obtained.

Since a single ended power supply was used, a blocking capacitor was needed in the output. The capacitor was chosen



to have a very low impedance (.02 ohms reactive) at 15 kilohertz. This corresponded to 500 microfarads. In this way with the capacitive reactance virtually negligible, undesirable phase shifts and voltage drop were virtually eliminated until on the brink of complete short circuit. The output transistor emitter resistors are of lower value than is customary in power circuit such as this (the usual value being from .25 to 1 ohm). The value of .1 ohm was chosen because of the necessity for having low internal impedance. The series feedback from these resistors inherently increases the output impedance. The loss in temperature stability and susceptibility to thermal runaway were compensated for by the current limiting ability of the power supply, a Power Designs Incorporated Model 3650 R which had the ability to current limit at any value from 0 to 5.5 amperes. Thermal problems were compensated for by careful attention to physical mounting and heat sinking of the transistors.

## 2. Selection of Output and Driver Transistors

For the output transistors, it was necessary to consider the expected continuous current drain on the source. Since this was on the order of five amperes the decision was made to use plastic silicon transistors for ease in mounting to a heat sink for good heat dissipation. Selection was also limited by availability in quantity (the process of matching requires a large stock to draw from). The resulting choices (MJE-2901 for the PNP and MJE-3055 for the NPN) were not the normally recommended complementary pair. However, their electrical similarity except for sign made them a likely prospect. A Tektronix type 576 curve tracer was used to examine the swept characteristics



of the transistors in question. It was found that the dynamic current gain,  $h_{fe}$ , of both types converged towards the same value (about 30) at high currents - on the order of five amperes. At lower quiescent currents it was found that the values from device to device varied considerably. Therefore, it was in this range, about 500 ma, that the output transistors were matched. When matching, careful attention was also paid to the slope of the curves (Emitter grounded,  $I_c$  vs.  $V_{ce}$  for stepped  $I_b$ ) beyond the knee (corresponding to  $1/h_{oe}$ ) and also  $V_{be}$  saturation voltage. The resulting pair were within 2% in all three parameters and virtually identical save for polarity.

For the drivers, the ability to deliver moderate currents, in the order of 200 milliamperes, and medium power dissipation, at least one watt, prompted the choice of 2N 3053 for the NPN and 40319 for the PNP. Once again, availability forced the use of not normally complemented devices. Great care with the curve tracer was also needed here.

It was found that  $h_{fe}$  did not vary drastically with increasing current carrying as in the output transistors, so the drivers were matched in the range from 50 to 250 milliamperes. As with the output transistors the parameters of  $h_{fe}$ ,  $V_{be}$  saturation voltage and  $1/h_{oe}$  were matched as closely as possible. The drivers were within the limits of the display accuracy of the curve tracer to being perfectly identical, within 1%.

### 3. Physical Consideration

For best possible heat dissipation and maintainance of close temperature similarity among the individual transistors all transistors were mounted to a common heat sink. Number





6-32 bolts were used to mount the output transistors to the heat sink. A slight improvement in conduction of heat away from the transistor was obtained by drilling and threading the holes in the heat sink to accept the 6-32 bolt rather than use a nut to hold everything secure. Very fine mica washers were used for insulation between the transistors and the heat sink but liberal amounts of silicone grease were used on all surfaces to keep thermal conductivity as high as possible.

The drivers, having TO-5 cases, were a little more difficult to mount. A socket like clip which would hold these transistors in an inverted position was obtained. This clip had a 6-32 lug on its base so the heat sink was drilled and tapped to accept them, the threads and mount were coated with silicone grease before mounting to the large heat sink.

The driver transistors were then coated with silicone grease and pressed into the clips. The grease prevented air gaps, so detrimental to heat flow, from becoming a problem. The overall assembly was capable of dissipating over 100 watts with only 70° centigrade rise in temperature above ambient. In addition, constant temperature from device to device was virtually 100% sure due to such close proximity and good thermal conductivity. Figure 2, Appendix A shows this arrangement.

## B. TESTING THE SOURCE

### 1. Distortion

The source was tested under various static loads of 5 ohms, 1 ohm and .2 ohms for distortion at maximum current, 5 amperes peak to peak. Distortion was checked by using a



Donner Wave Analyser Model 2102 to measure the amplitude of the expected harmonics in the waveform in the output. 15 kilohertz had to be used due to the limitation of 50 kilohertz on the wave analyser. The amplitude of the second harmonic was found to be .3% greater in the output than in the input waveform. Third harmonic content was .5% greater in the output than in the input at worse case.

## 2. Internal Impedance

Internal impedance was estimated by adjusting the source for one ampere peak to peak of current at one ohm load. The load was reduced to .2 ohm and the output voltage amplitude noted (.55 volts peak to peak). The load was then increased to 5 ohms and the output amplitude noted (1.2 volts peak to peak).

Internal impedance can then be determined by use of Ohm's law, assuming that the drive received from the signal generator is not altered by the change in load. The source can then be reduced to its Thevinin equivalent. Figure 3  
Appendix A.

From Ohm's law then, the output current is equal to the Thevinin voltage ( $V$ ) divided by the total circuit resistance ( $R_i + R_L$ ) which is also equal to output voltage ( $V_o$ ) divided by load resistance:

$$\frac{V}{R_i + R_L} = \frac{V_o}{R_L}$$



Substituting several values of  $V_o$  and  $R_L$  and solving for  $V$ :

$$V = \frac{V_{o1} (R_i + R_{L1})}{R_{L1}} = \frac{V_{L2} (R_i + R_2)}{R_{L2}}$$

which solved for  $R_i$  yields:

$$R_i = \frac{R_{Lo} R_{L2} (V_{o2} - V_{o1})}{R_{L2} V_{o1} - R_{L1} V_{o2}}$$

Substituting in the three values of  $R_L$  and  $V_o$  one gets an internal impedance of approximately .26 ohms.

From distortion and internal impedance data, the source was decided suitable for an actual ferroresonance study.



### III. THE SERIES RESONANT CIRCUIT

#### A. OBSERVATION OF THE PHENOMENON

The core chosen for study was an Indiana General CF-101-F core. (See Figure 4 Appendix A) 30 turns of number 34 wire were placed on the core to form an inductor. A capacitor of .1 microfarads was placed in series with the inductor and a signal of approximately 20 kilohertz was placed across this combination. The waveform of the source was monitored to check for distortion and the amplitude of the signal was increased while watching the inductor voltage. As the voltage across the circuit was increased, the circuit passed into classical ferro-resonance where the capacitor voltage waveform approximated a square wave. Increasing the voltage further brought a period of instability followed by transition into another stable mode. It was in this second mode that the asymmetrical behavior was noted. The capacitor voltage contained a strong third harmonic term. The inductor voltage was also highly asymmetrical, minor changes in amplitude effecting variation in the disparity of the period of the two halves of the waveform. With proper amplitude it was possible to realize a ratio of 2 to 1 between the periods of the positive going "half" cycle and the negative going "half" cycle with a marginal stability. The most stable inductor waveform is that of Figure 1 Appendix B. It was noted that in transitioning from instability to stability, as the voltage amplitude reached that necessary for stability, the stable asymmetric mode would assume the waveform in one of





two phases differing by  $180^\circ$ . Once one of the two phases was assumed by the circuit it was maintained until the input voltage amplitude was changed to take it out of the stable range. In addition, resumption of stability brought on the two phases in random fashion.

In order to pursue the study further it was desired to examine the dynamic hysteresis loop of the core. A second winding comprising five turns of number 30 wire was placed on the core. This winding was terminated in an R - C integrator consisting of a 100 kilohm resistor in series with a .5 microfarad capacitor. (Other values tried contained unbearable integration errors) Since the series combination was nearly totally resistive at the frequency in question, the voltage across the pair was proportional to the current in the winding which is proportional to magnetizing force. The voltage across the capacitor, on the other hand, is proportional to the integral of the winding current which is proportional to flux density. Placing these voltages on the horizontal and vertical channels respectively of an ANALAB Type 1100 two channel oscilloscope, a B - H loop was obtained as can be seen in Figure 2 of Appendix B. There are still serious integration errors in the loop, and the B - H loop shown is the optimum obtainable. The problem lay in the capacitor voltage being of such a small value compared to the voltage across the combination that the high amplification necessary in the oscilloscope to display it introduced distortion as well as delays in the waveform. Increasing the capacitance to resistance ratio resulted in errors due to improper integrator time constant for the frequency



used. Integrators using lower resistance values with high capacitances also excessively loaded the sense coil and reflected losses back to the inductor winding which altered the "Q" of the inductor. When this happened the waveform across the inductor was degraded and the stability of the asymmetric waveform suffered. In spite of the integration errors present and the degraded appearance of the B - H loop, one thing is quite obvious, there is a serious anomaly present. The hysteresis loop is definitely asymmetrical, there is a minor loop present. The minor loop cannot be due to the hysteretic properties of the core; however, it can be thought of as showing the history of the magnetization of the core through one cycle of its performance in the circuit under study. A close-up of the minor loop can be seen in Figure 3 Appendix B. Rudenburg has shown likely contours for minor loops during stable symmetrical modes of ferroresonance which give rise to high order subharmonics which can be seen in Figure 4 Appendix B. The loop present in Figures 2 and 3 are very similar to this hypothetical loop in spite of their degraded appearance. The asymmetry of the minor loop can be seen.

#### B. QUALITATIVE DESCRIPTION OF THE PHENOMENON

Taking the hypothetical hysteresis loop in Figure 6 and the corresponding waveforms in Figure 7, a qualitative description of the phenomenon can be given. Points 1, 2, 3 and 4 on the hysteresis loop correspond to  $t_1$ ,  $t_2$ ,  $t_3$  and  $t_4$  on the voltage waveforms. Starting at  $t_1$ , the input voltage is positive but decreasing, the capacitor voltage is relatively constant



and is greater than the input voltage. The voltage across the coil is  $V_{in} - V_c$ , the polarity is tending to drive the core to negative saturation. As the drive voltage goes negative this effect is increased until the core passes into negative saturation. Prior to the input voltage reaching its negative maximum the core saturates. At time  $t_2$  the capacitor voltage reverses polarity. This is due to two factors; the first being ferroresonant reversal of the inductor voltage, the second being the approaching arrival at negative maximum by the input voltage. The capacitor experiences the sum of these voltages and attempts to charge to nearly twice the input voltage through the low impedance of the saturated inductor. Once again the capacitor voltage exceeds input voltage and the inductor now sees a voltage of polarity tending to drive it toward positive saturation and now of a greater magnitude than that which drove it into negative saturation in the time from  $t_1$  to  $t_2$ . This drive increases until the input voltage reaches negative maximum where it then begins to decrease. Up to this point the rate of switching toward positive saturation has been much more rapid than the rate toward negative saturation previously, hence a more rapid arrival at positive saturation by the core. At  $t_3$  the input waveform is reaching zero and at the same time the inductor is undergoing another ferroresonant reversal. The capacitor tries to charge to this voltage, but since the drive voltage is zero the charging rate is slower and since the core was not aided by the drive voltage the reversal is slower. Since the sides of the B - H loop are not vertical,



(indicating a less than infinite impedance) the capacitor sees a finite impedance to discharge through. However, the rising input voltage slows this discharge and the capacitor voltage levels off. Now at  $t_4$ , the capacitor voltage exceeds the input voltage, the core once again heads toward negative saturation; however, before this process can get well underway the input voltage exceeds the capacitor and the core tries to change directions and move into positive saturation. Before this process can reach completion the input voltage has reached its positive maximum and began to decrease. It is this chain of events after  $t_4$  which account for the minor loop. As the input voltage decreases below the capacitor voltage, the cycle is completed and the loop finished. The cycle can now begin again.

### C. QUANTITATIVE DESCRIPTION OF PHENOMENON

#### 1. Circuit Equations

By Faraday's law, the voltage across the coil is equal to  $N \frac{d\phi}{dt}$ .

The entire circuit is governed by the integrodifferential equation:

$$N \frac{d\phi}{dt} + R_i + \frac{1}{C} \int i dt = - E \cos \omega t \quad (1)$$

where  $\phi(0) = \phi_0$ ,  $i(0) = 0$ ,  $\omega = 2\pi \times 2.1 \times 10^4$  and where  $R$  is the circuit impedance.

In Reference 1, Dennard shows the development of an equation for  $i(t)$  from a plot of  $\phi$  vs.  $i$  for the circuit. Two points on the curve were used,  $(6.2 \times 10^{-7}, 0.15)$  and  $(2.0 \times$





$10^{-7}$ , 0.03). These were substituted to the general cubic equation:

$$i = b_1 \phi + b_3 \phi^3 \quad (2)$$

Simultaneous solution of the two resulting equations gave

$$i = 1.46 \times 10^5 \phi + 3.78 \times 10^{17} \phi^3 \quad (3)$$

$$b_1 = 1.46 \times 10^5 \quad b_3 = 3.78 \times 10^{17}$$

After insertion of the values into the circuit equation and differentiation to remove the integral, the result using operator notation is:

$$D^2 + \frac{Rb_1}{N} D + \frac{b_1}{NC} \phi + \frac{Rb_3}{N} D + \frac{b_3}{NC} \phi^3 = \frac{\omega E}{N} \sin \omega t \quad (4)$$

To separate the constant flux component,  $\phi_0$ , a new variable is defined:

$$x(t) = \phi(t) - \phi_0 \quad (5)$$

This change of variable allows (4) to be rewritten as:

$$\begin{aligned} (D^2 + K_1 D + K_2)X + 3\phi_0(K_4 D + K_3)X^2 + (K_4 D + K_3)X^3 = \\ - K_5 + K_6 \sin \omega t \end{aligned} \quad (6)$$



where

$$K_1 = \frac{Rb_1 + 3\phi_o^2 Rb_3}{N}$$

$$K_2 = \frac{b_1 + 3\phi_o^2 b_3}{NC}$$

$$K_3 = \frac{b_3}{NC}$$

$$K_4 = \frac{Rb_3}{N}$$

$$K_5 = \frac{b_3\phi_o^2 + b_1\phi_o}{NC}$$

$$K_6 = \frac{\omega E}{N}$$

From reference 1,  $\phi_o$  is approximately  $3.0 \times 10^{-8}$  webers. The effect of  $\phi_o$  upon the terms in which it is contained in powers greater than one is negligible, therefore, the following approximations are in order.

$$K_1 \approx \frac{Rb_1}{N} = 1.95 \times 10^4$$

$$K_2 \approx \frac{b_1}{NC} = 4.87 \times 10^{10}$$

$$K_3 \approx \frac{b_2}{NC} = 1.26 \times 10^{23}$$

$$K_4 \approx \frac{Rb_3}{N} = 5.05 \times 10^{16}$$



$$K_5 \approx \frac{b_1 \phi_0}{NC} = 1.5 \times 10^3$$

$$K_6 \approx \frac{E\omega}{N} = 2.2 \times 10^4$$

If the following changes are made:

$$a_1 = D^2 + K_1 D + K_2$$

$$a_2 = 3\phi_0 (K_4 D + K_3)$$

$$a_3 = K_4 D + K_3$$

equation (6) can be rewritten as:

$$a_1 X + a_2 X^2 + a_3 X^3 = -K_5 - K_6 \sin \omega t \quad (7)$$

A solution for this equation in terms of  $X(t)$  can be obtained by the method of reversion of series [Ref. 2].

Reversion of series is a method of solving ordinary nonlinear differential equations. The method is based on the algebraic procedure in reversing power series.

The nonlinear differential equation can be written as (in the notation of Reference 2):

$$a_1 y + a_2 y^2 + a_3 y^3 + \dots = K \phi(t) \quad (8)$$

where  $t$  is the independent variable,  $y$  is the desired dependent variable,  $K$  is a constant, and  $\phi(t)$  is a given function. The  $a_i$  coefficients are, in general, operators.



Assuming a solution of the form:

$$y = A_1 K + A_2 K^2 + A_3 K^3 + \dots \quad (9)$$

The  $A_i$ 's are determined by substituting (9) into (8) and equating coefficients of equal powers of  $K$ . This yields:

$$A_1 = \phi t / a_1 \quad (10)$$

$$A_2 = -a_2 A_1^2 / a_1 \quad (11)$$

$$A_3 = -(1/a_1) (2a_2 A_1 A_2 + a_3 A_1^3) \quad (12)$$

Equation (7), having been developed towards a solution by reversion of series, is in proper format if  $K = 1$  and  $\phi(t) = -K_5 + K_6 \sin \omega t$ . The solution is then of the form:

$$X(t) = A_1(t) + A_2(t) + A_3(t) \quad (13)$$

Taking the derivative gives the voltage across the coil.

$A_1$ , the initial term of (13), is found by solving the following equation for  $A_1(t)$

$$a_1 A_1(t) = -K_5 + K_6 \sin \omega t \quad (14)$$

The operator  $a_1$  appears in the solution of each  $A_i$  and is therefore the most influential element in the solution.

The roots of  $a_1$  are:

$$D = -\frac{K_1}{2} \pm \frac{j}{2} \sqrt{4K_2 - K_1^2}$$





$$\text{Let: } \alpha = \frac{K_1}{2}, \quad \beta = \frac{1}{2} \sqrt{4K_2 - K_1^2} \approx K_2$$

$$\beta_o^2 = \alpha^2 + \beta^2 = K_2 \quad (15)$$

$a_1$  can then be rewritten as:

$$a_1 = D^2 + K_1 D + K_2 = (D + \alpha)^2 + \beta^2 \quad (16)$$

Taking the Laplace Transform of (14) yields:

$$A_1(s) = \frac{-K_5}{s[(s+\alpha)^2 + \beta^2]} + \frac{K_6 \omega}{(s^2 + \omega^2)[(s+\alpha)^2 + \beta^2]} \quad (17)$$

Direct transform pairs from Reference 3 gives:

$$\begin{aligned} A_1(t) = & \left[ \frac{1}{\beta_o} + \frac{1}{\beta_o \beta} e^{-\alpha t} \sin(\beta t - \psi_1) \right] + \\ & K_6 \omega \frac{1}{[(\beta_o^2 - \omega^2)^2 + 4\alpha^2 \omega^2]^{1/2}} \left[ \frac{1}{\omega} \sin(\omega t - \psi_2) \right. \\ & \left. + \frac{1}{\beta} e^{-\alpha t} \sin(t - \psi_3) \right] \quad (18) \end{aligned}$$

$$\text{where } \psi_1 = \tan^{-1} \frac{\beta}{-\alpha} \approx \frac{\pi}{2}$$

$$\psi_2 = \tan^{-1} \frac{2\alpha\omega}{\beta_o^2 - \omega^2} \approx 0$$

$$\psi_3 = \frac{-2\alpha\beta}{\alpha^2 - \beta^2 + \omega^2} \approx \pi$$



$$A_1(t) \approx -K_1 + e^{-\alpha t} [K_1 \cos \beta t - \frac{K_2}{\beta} \sin \beta t] + \frac{K_2}{\omega} \sin \omega t \quad (19)$$

where  $K_1 = 3.08 \times 10^{-7}$

$$K_2 = 9.28 \times 10^{-2}$$

It can be noted that there appear exponential terms as well as the sine and cosine terms. Since only the steady state solution was of interest here, all exponential terms were excluded from the solution and do not appear in following expressions.

By similar attack,  $A_2$  was evaluated and found to consist of terms of very small magnitude (the largest being  $10^{-13}$ ); therefore,  $A_2$  was not considered necessary to the solution.

The defining equation for  $A_3$  can be written:

$$a_1 A_3 = -a_3 [6\phi_0 A_1 A_2 + A_1^3] \quad (20)$$

Since it was determined previously that  $A_1$  is greater than  $A_2$ , term for term, by several orders of magnitude. Therefore  $6\phi_0 A_1 A_2$  is less than  $A_1^3$ , term by term by an equivalent amount. Equation (20) can therefore be approximated by:

$$a_1 A_3 \approx -a_3 A_1^3 \quad (21)$$



After removal of the decaying exponential terms,  $A_3$  is found to be:

$$A_3 = 7.4 \times 10^{-8} - 1.5 \times 10^{-6} \sin (\omega t - .093) + 0.87 \times 10^{-8} \sin 3 \omega t \quad (22)$$

$A_1$  after the removal of unnecessary exponential terms is:

$$A_1 = - 3.08 \times 10^{-7} + \frac{9.28 \times 10^{-2}}{\omega} \sin \omega t \quad (23)$$

The solution for the voltage across the inductor is obtained by taking the sum of equations (22) and (23), taking the derivative of the combination and then multiplying by the number of turns. The result is:

$$V_L = N[-8 \times 10^{-7} \omega \cos (\omega t - .0930) + 9.87 \times 10^{-9} (3\omega) \cos 3\omega t] \quad (24)$$

Substitution of values into this formula through one cycle yields the waveform shown in Figure 5 Appendix B.



#### IV. CONCLUSION

A comparison of Figures 1 and 5 of Appendix B shows the analysis to be rather accurate. There are obviously higher order terms than third harmonic in the inductor wave form. The unequal size of the positive "humps" and also the inequality of the period of these two humps confirms this fact. Another factor causing inaccuracy may well be stray impedances (resistive), that could not be eliminated. Introduction of a .2 ohm resistor into the series coil-capacitor circuit caused an increase in this disparity; further decreasing the circuit impedance should cause the opposite to happen. This could be accomplished by further reduction in source impedance (which would be difficult with present semiconductor technology) or by larger wire for the coil winding, or by use of a higher quality capacitor with a much lower dissipation factor. Actually, a combination of all three would be necessary here since any one could only effect very minor changes (measured in hundredths of an ohm) in the overall circuit impedance.

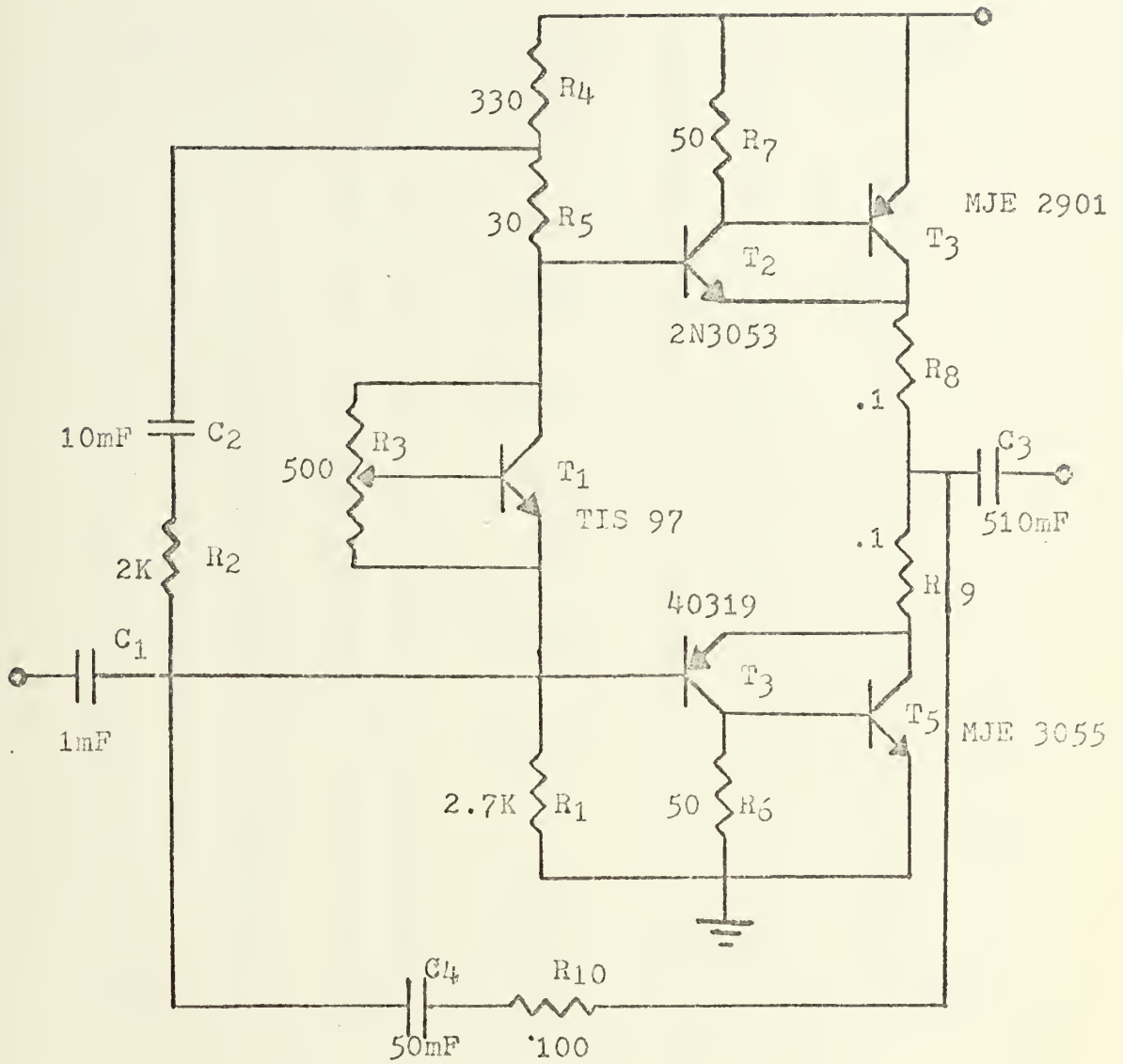
In designing the source, the minimum specifications to be met were 2% distortion and less than .5 ohm internal impedance. The source as tested was 50% lower in both these categories.

All factors considered, the source performed very well, the standards of low distortion and low internal impedance were met and allowed a successful study of a complex phenomenon to be performed with good results.





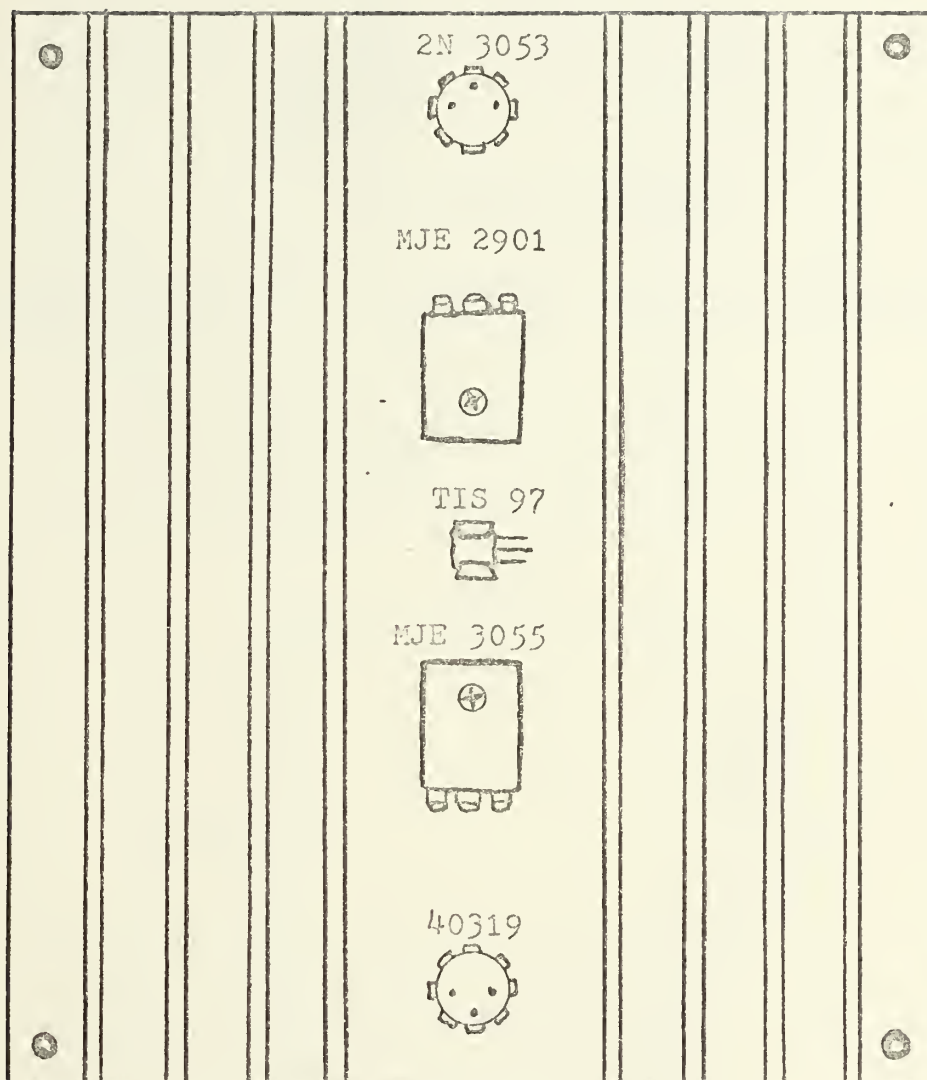
# APPENDIX A



Circuit diagram of Source

Figure 1



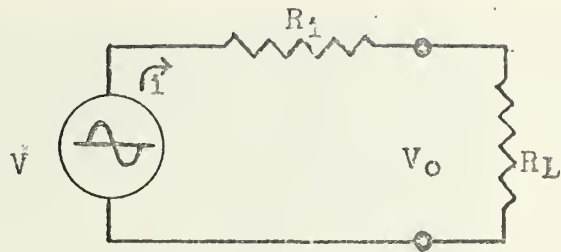


SCALE : FULL

Physical mounting on heatsink

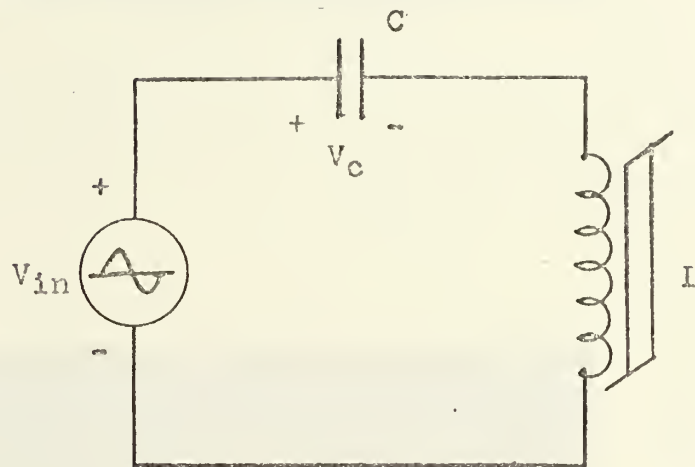
Figure 2





Thevenin equivalent of the Source for internal impedance calculation.

Figure 3



Ferroresonant Circuit

$V_{in}$  = 0 to 10 volts pp  
15 to 25 KHz

$C$  = .1 microfarads

$L$  = 30 turns on Indiana General  
CF-101-F core

Core

I.D. = .12"

O.D. = .23"

Ht. = .06"

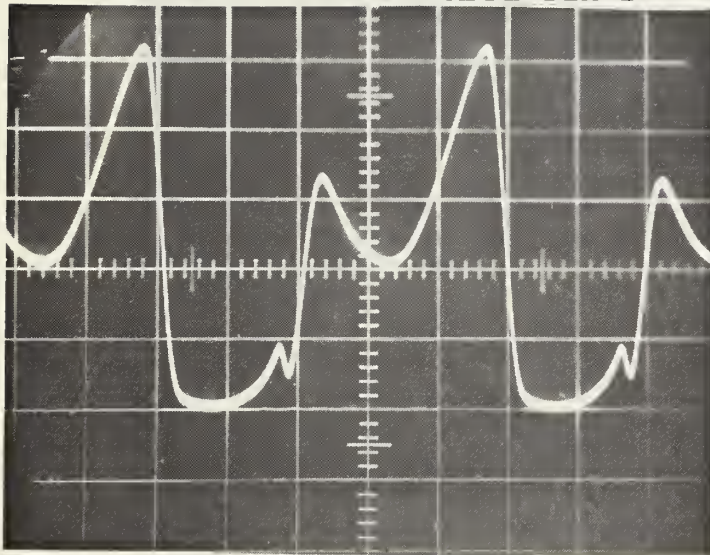
$B_s$  = 3.4 KG  $B_r$  = 1.47 KG

$H_c$  = .18 Oe

Figure 4



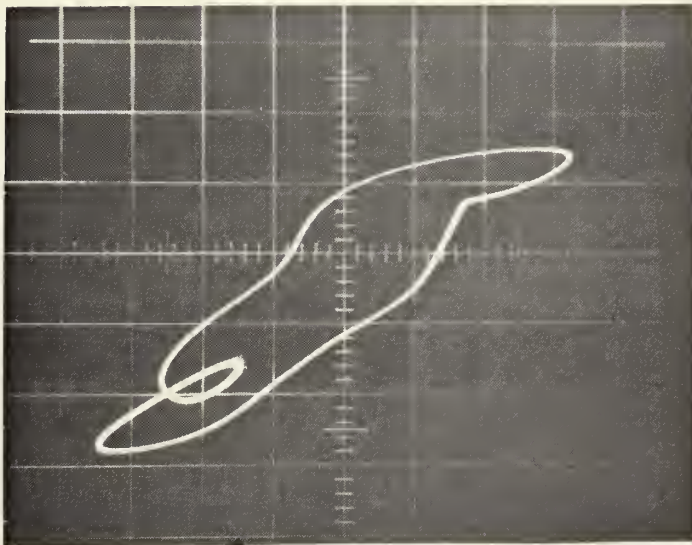
APPENDIX B



Vertical  
.5 volts/cm  
Horizontal  
.05 msec/cm

Inductor Waveform

Figure 1



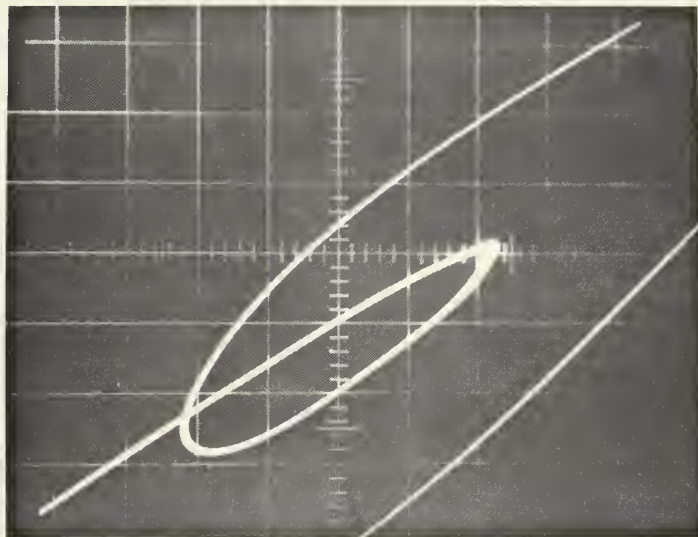
Vertical  
2 mvolts/cm  
Horizontal  
10 ma/cm

Hysteresis Loop

Figure 2







Vertical = 1 mV/cm

Horizontal = 2. mA/cm

Expansion of minor loop

Figure 3

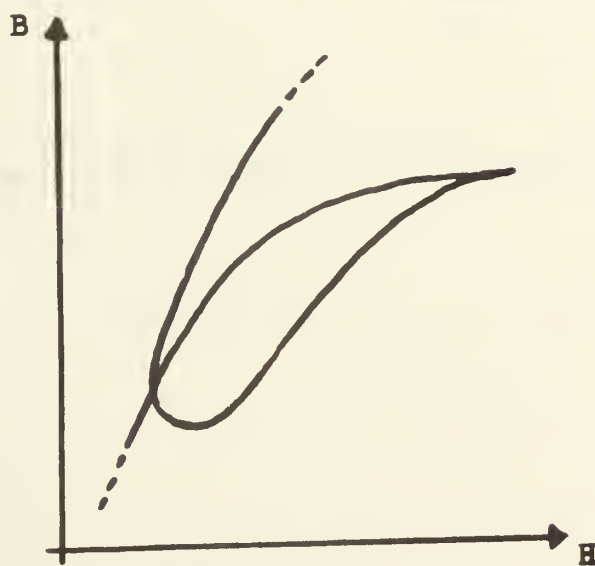
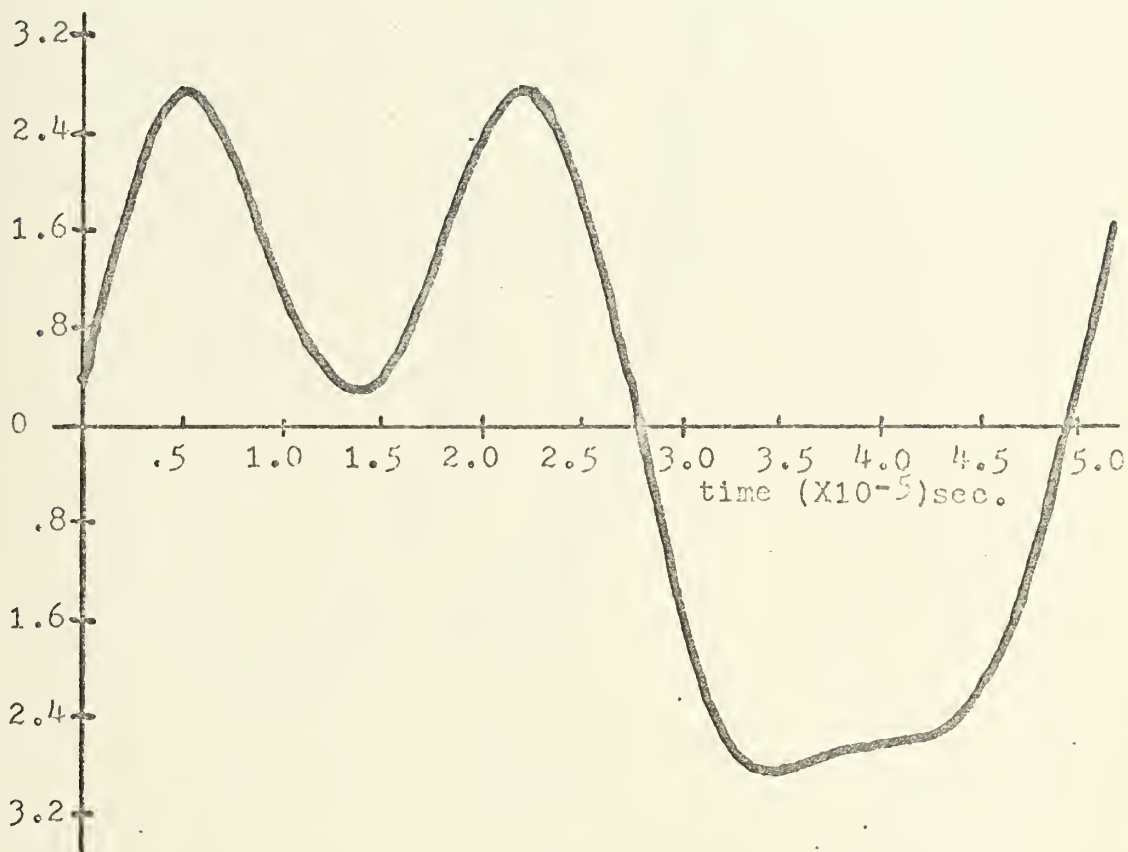


Figure 4

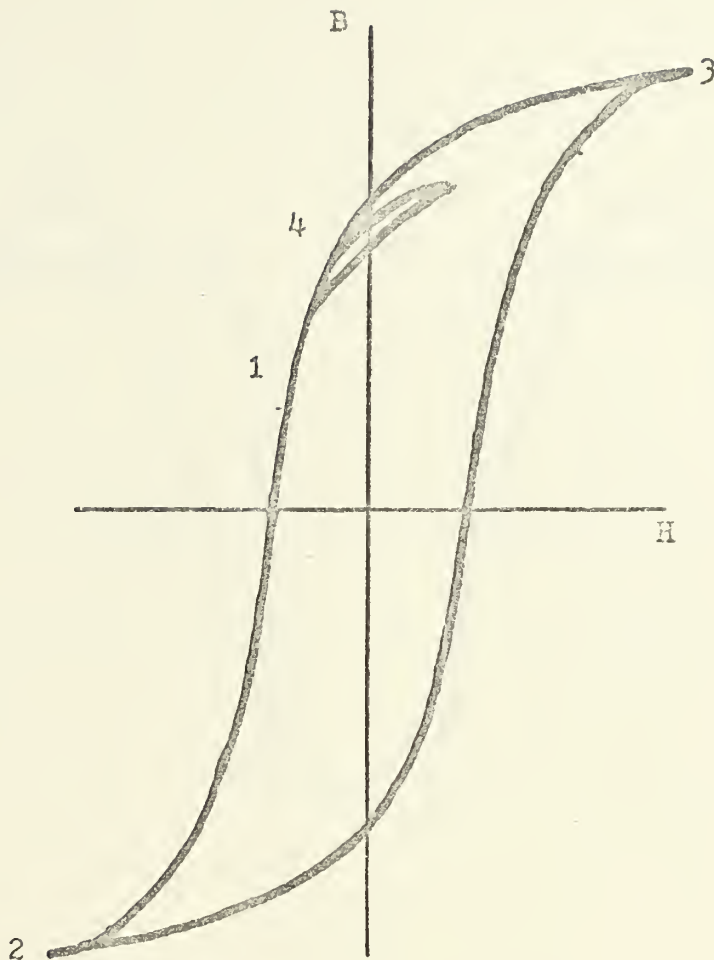




Theoretical Waveform for Inductor

Figure 5

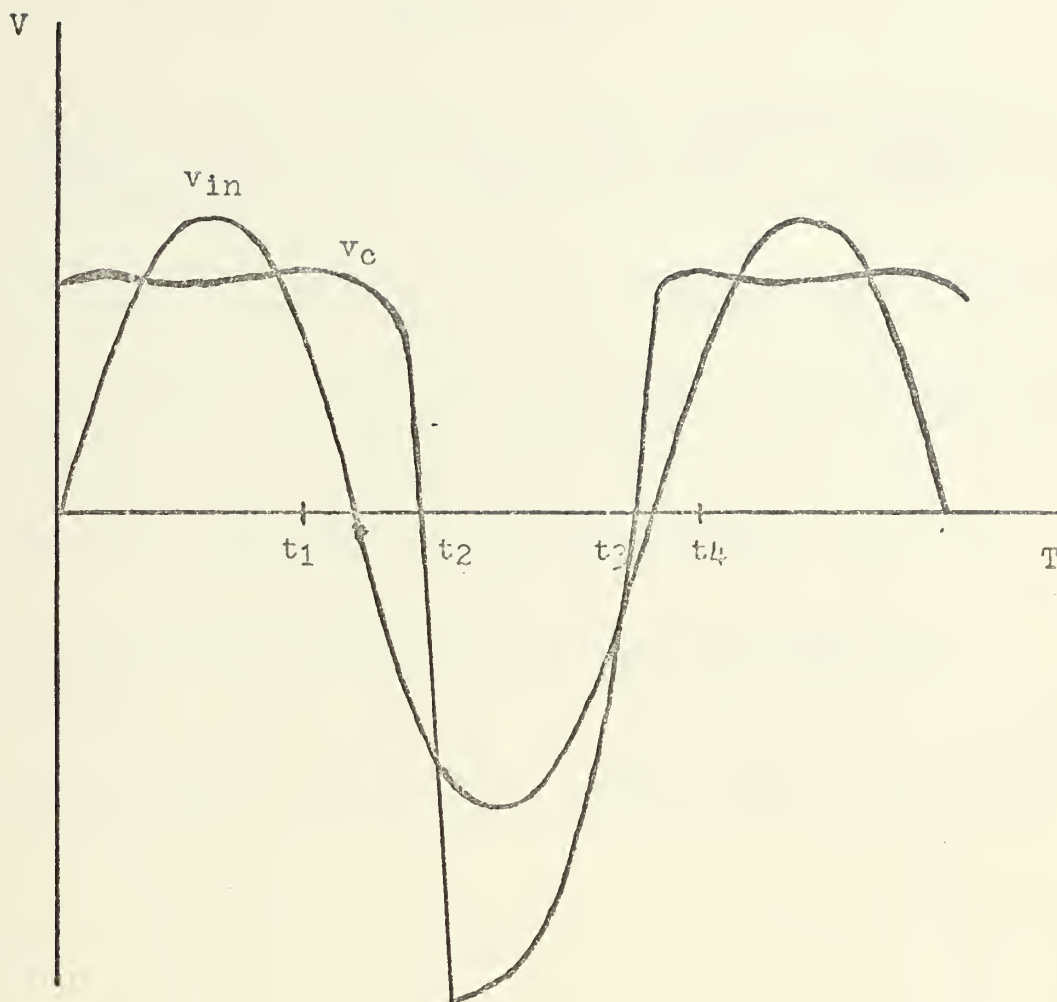




Hysteresis loop for qualitative description of the ferroresonance phenomenon.

Figure 6





Input and capacitor voltages for qualitative description of the ferreresonance phenomenon.

Figure 7





## BIBLIOGRAPHY

1. R. H. Dennard, "Behavior of The Ferroresonant Series Circuit Containing a Square-Loop Reactor," AIEE Transactions, Pt. 1 (Communications and Electronics), Vol 77, pp.903-911, 1958.
2. R. P. Evans, "Series Circuit Incorporating a Nonlinear Reactor," AIEE Conference Paper 56-683, June, 1956.
3. L. A. Pipes, "The Reversion Method for Solving Nonlinear Differential Equations," Journal of Applied Physics, Vol. 33, No. 2, pp.202-207, 1952.
4. R. Rudenberg, "Nonharmonic Oscillators as Caused by Magnetic Saturation," AIEE Transactions, Vol. 68, Pt. 1, pp.676-685, 1949.
5. L. G. Cowles, Analysis and Design of Transistor Circuits, pp.181-198, D. Van Nostrand Co., Inc., 1966
6. F. C. Fitchen, Transistor Circuit Analysis and Design, pp.183-203, D. Van Nostrand Co., Inc., 1966.



# INITIAL DISTRIBUTION LIST

	No. Copies
1. Defense Documentation Center Cameron Station Alexandria, Virginia 22314	2
2. Library, Code 0212 Naval Postgraduate School Monterey, California 93940	2
3. Assoc. Professor O. M. Baycura, Code 52 Department of Electrical Engineering Naval Postgraduate School Monterey, California 93940	1
4. LT(jg) John R. Pratchois, USN 307 Nimitz Avenue Rockville, Maryland 20851	1



## DOCUMENT CONTROL DATA - R &amp; D

(Security classification of title, body of abstract and indexing annotation must be entered when the overall report is classified)

1. ORIGINATING ACTIVITY (Corporate author) Naval Postgraduate School Monterey, California 93940		2a. REPORT SECURITY CLASSIFICATION Unclassified	
		2b. GROUP	
3. REPORT TITLE A Low Impedance High Current Ultrasonic Signal Source for Ferroresonance Study			
4. DESCRIPTIVE NOTES (Type of report and, inclusive dates) Master's Thesis; September 1970			
5. AUTHOR(S) (First name, middle initial, last name) John Reynolds Pratchios			
6. REPORT DATE September 1970		7a. TOTAL NO. OF PAGES 37	7b. NO. OF REFS 6
8a. CONTRACT OR GRANT NO.		9a. ORIGINATOR'S REPORT NUMBER(S)	
b. PROJECT NO.			
c.		9b. OTHER REPORT NO(S) (Any other numbers that may be assigned this report)	
d.			
10. DISTRIBUTION STATEMENT This document has been approved for public release and sale; its distribution is unlimited.			
11. SUPPLEMENTARY NOTES		12. SPONSORING MILITARY ACTIVITY Naval Postgraduate School Monterey, California 93940	
13. ABSTRACT <p>In ferroresonant mode, a transformer is saturated and requires very high currents from the source. Previous studies of ferroresonance could not be performed effectively because of high internal impedance of the source. Introduction of transformers to improve these shortcomings would have also introduced undesirable inductive effects. In this thesis, a transistor voltage source with low internal impedance and high current delivering ability is designed and tested. The source is used to investigate an unsymmetrical mode of series resonance. Resonant circuit behavior is both qualitatively and quantitatively described.</p>			



## KEY WORDS

## LINK A

## LINK B

## LINK C

ROLE

WT

ROLE

WT

ROLE

WT

Ferroresonance

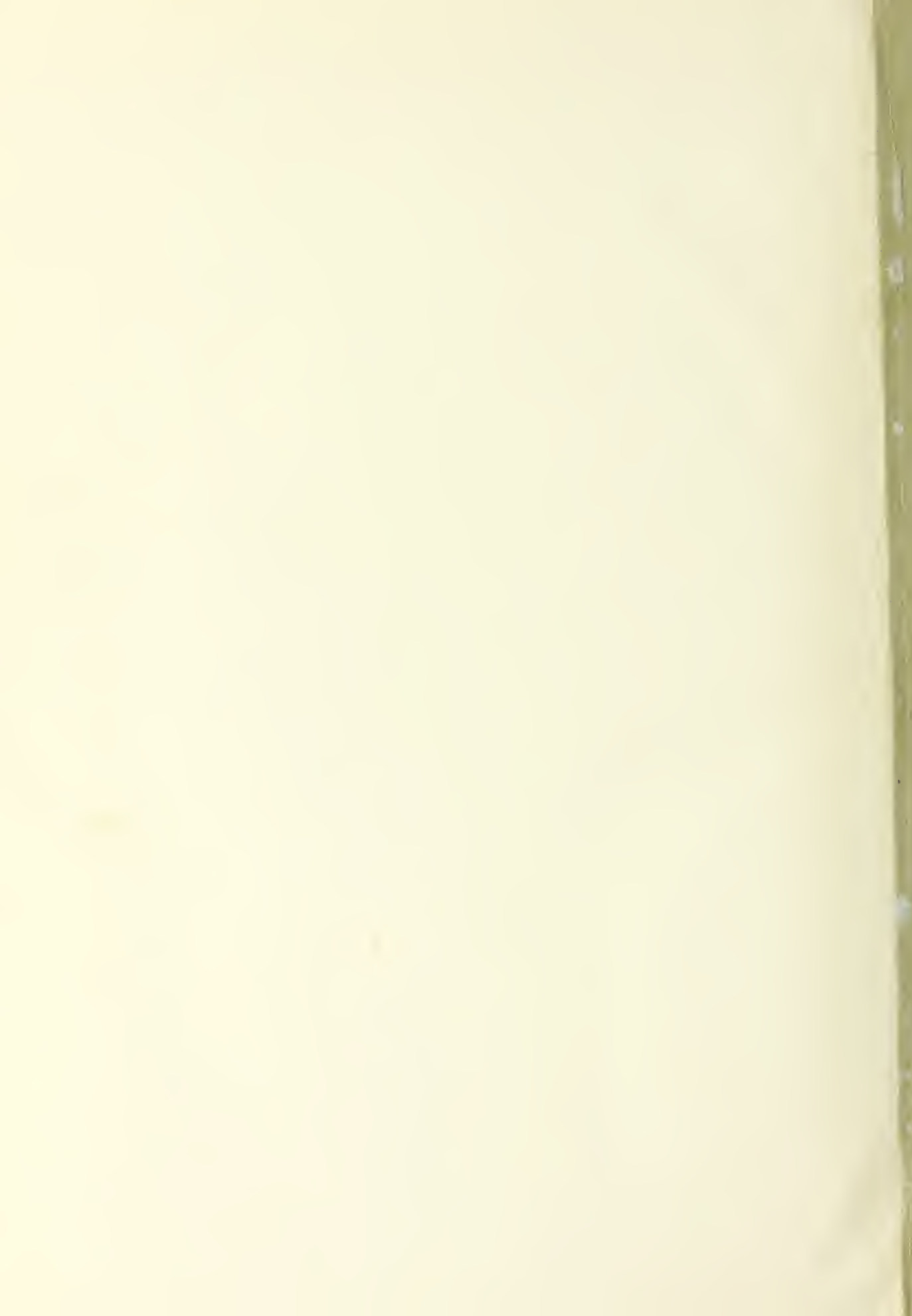
Transistor

Amplifiers









Thesis  
P82  
c.1

Pratchios

124437

A low impedance  
high current ultra-  
sonic signal source  
for ferroresonance  
study.

Thesis  
P82  
c.1

Pratchios

124437

A low impedance  
high current ultra-  
sonic signal source  
for ferroresonance  
study

thesP82

A low impedance high current ultrasonic



3 2768 000 99535 1

DUDLEY KNOX LIBRARY